



INSTITUT DE FRANCE
Académie des sciences

Comptes Rendus

Géoscience

Sciences de la Planète


Mo Wuling, Fan Liyong, Wei Guoqi, Liu Xinshe, Zhang Chunlin, Liu Mancang, Su Nan, Liu Yan, Wu Saijun and Xing Fengcun

Detrital zircon U–Pb geochronology from the Upper Carboniferous sediments of Benxi Formation in the North China Craton: implications for tectonic-sedimentary evolution

Volume 352, issue 2 (2020), p. 169-184

Published online: 4 November 2020

<https://doi.org/10.5802/crgeos.17>

 This article is licensed under the
CREATIVE COMMONS ATTRIBUTION 4.0 INTERNATIONAL LICENSE.
<http://creativecommons.org/licenses/by/4.0/>



*Les Comptes Rendus. Géoscience — Sciences de la Planète sont membres du
Centre Mersenne pour l'édition scientifique ouverte*

www.centre-mersenne.org

e-ISSN : 1778-7025



Tectonics, Tectonophysics — Original Article

Detrital zircon U–Pb geochronology from the Upper Carboniferous sediments of Benxi Formation in the North China Craton: implications for tectonic-sedimentary evolution

Mo Wuling[Ⓢ]*, ^a, Fan Liyong^b, Wei Guoqi^a, Liu Xinshe^b, Zhang Chunlin^a, Liu Mancang^a, Su Nan^a, Liu Yan^b, Wu Saijun^a and Xing Fengcun^c

^a Research Institute of Petroleum Exploration & Development, Beijing, 100083, China

^b Exploration and Development Research Institute of PetroChina Changqing Oil field Company, Xi'an 710018, China

^c Chengdu University of Technology, Chengdu 610059, China

E-mails: mow150@petrochina.com.cn (M. Wuling), lyfan123_cq@petrochina.com.cn (F. Liyong), weigq@petrochina.com.cn (W. Guoqi), lxs_cq@petrochina.com.cn (L. Xinshe), zhangcl69@petrochina.com.cn (Z. Chunlin), liumc69@petrochina.com.cn (L. Mancang), sunan11a23@petrochina.com.cn (S. Nan), liuyan01_cq@petrochina.com.cn (L. Yan), wusaijun@petrochina.com.cn (W. Saijun), 57651298@qq.com (X. Fengcun)

Abstract. The provenance of the Upper Carboniferous Benxi Formation in North China Craton (NCC) has been considered as the northern margin of the NCC, not the North Qinling Orogenic Belt. To understand the provenance and the tectonic-sedimentary evolution during the sedimentary period of the Benxi Formation, the zircon U–Pb geochronology analysis was conducted on eleven clastic sandstone samples. The south of the NCC received clastic sediments from the North Qinling Orogenic Belt. The orogenic movements around the NCC in the Late Carboniferous period had significant impacts on the changes in paleotopography. During the early sedimentary period of the Hutian member of the Benxi Formation, the north of the Qinling Orogenic Belt was rapidly uplifted, and paleotopography was south-uplifting and north-dipping; thus, the clastic source was the North Qinling Orogenic Belt. From the late sedimentary period of the Benxi Formation Hutian member to the sedimentary period of the Jinci member, paleotopography was reversed. The northern margin of the NCC quickly uplifted, and paleotopography was north-uplifting and south-dipping. Two distinct provenances were present in the sediments of the Benxi Formation. The sediments were supplied predominately by the provenance in the north.

Keywords. North China Craton, North Qinling Orogenic Belt, Carboniferous Benxi Formation, U–Pb chronology of detrital zircon, Tectonic-sedimentary evolution.

Manuscript received 15th March 2020, revised 26th May 2020, accepted 23rd July 2020.

* Corresponding author.

1. Introduction

The North China Craton (NCC) is bordered to the north by the Bainaimiao arc, located in the southern part of the Central Asian Orogenic Belt [Xu *et al.*, 2013, Zhang *et al.*, 007a,b, Faure *et al.*, 2007, Shi *et al.*, 013a,b], and to the south by the North Qinling arc in the North Qinling Orogenic Belt (Figure 1) [Chen, 1998, Mattauer *et al.*, 1985, Wang *et al.*, 2016, Zhu *et al.*, 2007]. During the Palaeozoic era, the NCC witnessed a sedimentary hiatus of ca. 150 Ma from the Middle Ordovician to the Late Carboniferous. The Benxi Formation (of the Pennsylvanian system) deposited a set of clastic-dominated stratum on the Ordovician carbonate strata.

Most studies have supported the presence of a fluvial-delta sedimentary system in the northern part of the NCC and a lagoon-barrier island sedimentary system in the southern part during the Late Carboniferous Benxi Formation [Chen *et al.*, 2010, Li *et al.*, 2014, Shao *et al.*, 2014, Zhu *et al.*, 2007].

Those studies have considered the northern margin of the NCC as the provenance for sandstone and conglomerates of the barrier island system. Hou *et al.* [2018] showed that the Carboniferous Benxi Formation was the tidal-delta complex facies associations in the northern part of the NCC, and the sand body indicating that the delta was developed in the southern part of the NCC. Jia *et al.* [2019] demonstrated that there was a main provenance system in the northern and southern parts of the NCC. The northern provenance supply was obvious and dominant.

The karst-type bauxites commonly contain abundant detrital zircon [Deng *et al.*, 2010] that can be used to study the sedimentary provenance and tectonic evolution of source regions [Cawood *et al.*, 2012]. Attempts have been made to study the zircon U–Pb age of bauxite [Cai, 2014, Wang *et al.*, 2016], which suggests that detrital zircon in the Late Carboniferous bauxite might be sourced from the mountains at the northern and southern margins of the NCC. However, no research has been conducted on detrital zircon U–Pb geochronology for sandstone samples recovered from the middle and upper parts (the Pangou and Jinci members) (Figure 2) of the Benxi Formation in the southern part of the NCC. In general, there is a series of problems with regard to the Late Carboniferous Benxi period in the NCC, such as the regional tectonic environment, source of

sediments, and evolution of the North Qinling Orogenic Belt. In this study, we collected sandstone samples in the Benxi Formation with abundant detrital zircons and combined the data with the results of the previous studies on zircon U–Pb geochronology in bauxite at the bottom of the Benxi Formation. We then conducted zircon U–Pb geochronology and Hf isotope analysis. Finally, we discussed the source of detrital zircons in the Benxi Formation sediments deposited in the NCC, and the tectonic-sedimentary evolution of the provenance, thereby providing new data for the study of basin-mountain coupling relationship and the natural gas exploration of the Benxi Formation.

2. Geologic setting

The basement of the NCC consists of three microcontinental blocks (Eastern Block, Yinshan Block, and Ordos Block) and three Paleoproterozoic mobile belts (Khondalite Belt, Trans-North China Orogen, and Jiao-Liao-Ji Belt). The Ordos Block and the Yinshan Block collided along the East-West Khondalite Belt at ~1.95 Ga, which formed the West Block. Then, the West Block collided with the East Block along the Trans-North China Orogen at ~1.85 Ga, which formed a unified crystalline basement of the NCC [Faure *et al.*, 2007, Zhai, 2007]. After the completion of cratonization, the NCC was in a stable platform until the early Mesozoic, and formed a thick sedimentary caprock of Meso- and Neo-Proterozoic and Phanerozoic. Intrusive rock are reported from the northern margin of the NCC, as well as a few metamorphic rock outcrops. Their zircon ages range from 300 to 330 Ma, peaking at ca. 310 Ma [Shi *et al.*, 013a,b, Zhang *et al.*, 2004, 006a, 007a,b, 2011].

The North Qinling Orogenic Belt is situated between the Luo-Luan fault belt and Shangdan suture belt [Meng and Zhang, 2000]. Multiple episodes of intrusions and dikes occurred in the North Qinling Orogenic Belt, whose age ranges from 400 to 500 Ma and peaks at ca. 450 Ma [Chen *et al.*, 2007, Guo *et al.*, 2010, Jiang *et al.*, 2009, Lerch *et al.*, 1995, Li *et al.*, 2008, Lu *et al.*, 2003, Pei *et al.*, 2007, Sun, 1991, Tian, 2003, Wang *et al.*, 2009, Wen *et al.*, 2008, Xu *et al.*, 2008, Xue *et al.*, 1996, Yan *et al.*, 2007, Zhang *et al.*, 006b]. The intrusions and dikes in the North Qinling Orogenic Belt present the geochemical features of arc terranes. Li [2011] suggested that the Early Palaeozoic

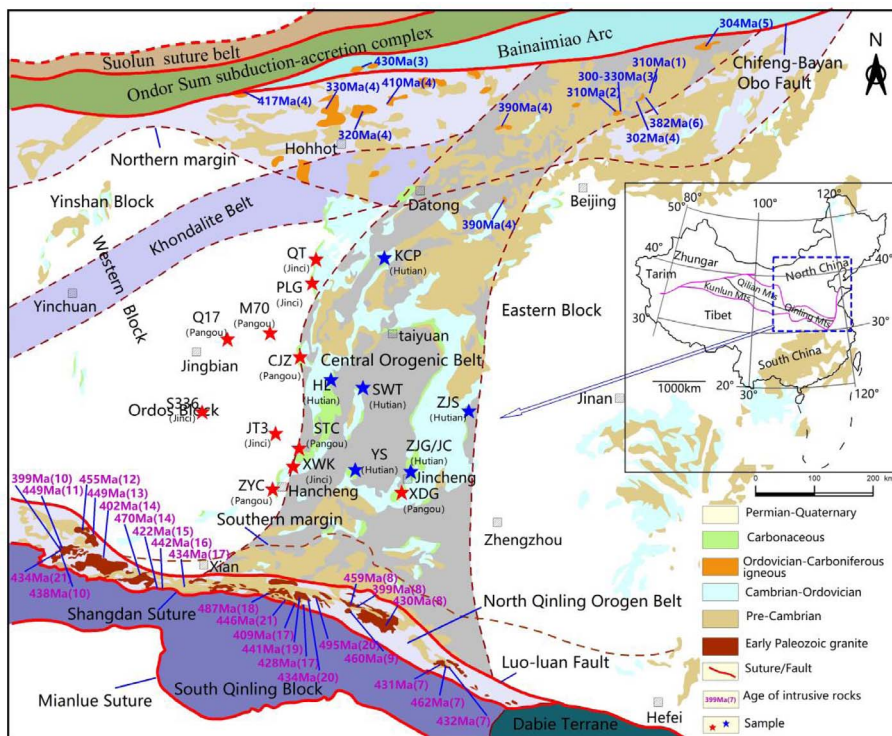


Figure 1. Regional geological map of the North China Craton. The zircon U–Pb age data shown in this map are from (1) Zhang et al., 2004; (2) Zhang et al., 2007a; (3) Zhang et al., 2007b; (4) Zhang et al., 2011; (5) Zhang et al., 2006a; (6) Shi et al., 2013a,b; (7) Jiang et al., 2009; (8) Tian, 2003; (9) Guo et al., 2010; (10) Wen et al., 2008; (11) Pei et al., 2007; (12) Chen et al., 2007; (13) Xu et al., 2008; (14) Xue et al., 1996; (15) Lerch et al., 1995; (16) Yan et al., 2007; (17) Lu et al., 2003; (18) Sun, 1991; (19) Li et al., 2008; (20) Wang et al., 2009; (21) Zhang et al., 2006b. The red marked locations are the sampling sites in this study. The blue marked locations are from Cai (2014) (KCP, HL, SWT, YS, ZJG, JC), Wang et al. [2016] (ZJS).

Era ocean basin in North Qinling developed into a mature ocean (ca. 514 Ma) before the Late Cambrian. When the ocean basin was completely closed, the continent-continent collision continued through the Late Devonian or Early Carboniferous (ca. 350 Ma) for about 160 Ma.

The southern Central Asian Orogenic Belt is composed of the Ondor Sum subduction-accretion complex and the Bainaimiao arc terrane [Zhu et al., 2007]. The Ondor Sum subduction-accretion complexes contain turbidite, high-pressure mylonite, and blueschist. The $^{39}\text{Ar}/^{40}\text{Ar}$ age of the glaucophane in the blueschist ranges from 446 ± 15 to 426 ± 15 Ma [De Jong et al., 2006]. The age of the Early-Middle Ordovician volcanic rock in the Bainaimiao arc is determined using biostratigraphy. Intrusive rocks of ca.

450 Ma are widespread in this area [Li et al., 2012]. The Late Silurian conglomerate, neritic clastic sedimentary rock, and carbonate rock overlaid unconformably the Bainaimiao arc. In the late Carboniferous, the arc was reactivated by the southward subduction of the Paleo-Asian Ocean to form the mafic-felsic volcanic rocks.

3. Geological features of the Carboniferous Benxi Formation

The Benxi Formation was deposited at the initial period of the Late Paleozoic in the NCC, as a result of the transgression of the North China Sea from the northeast. The Benxi Formation was deposited in the weathering crust of the Ordovician in the Lower

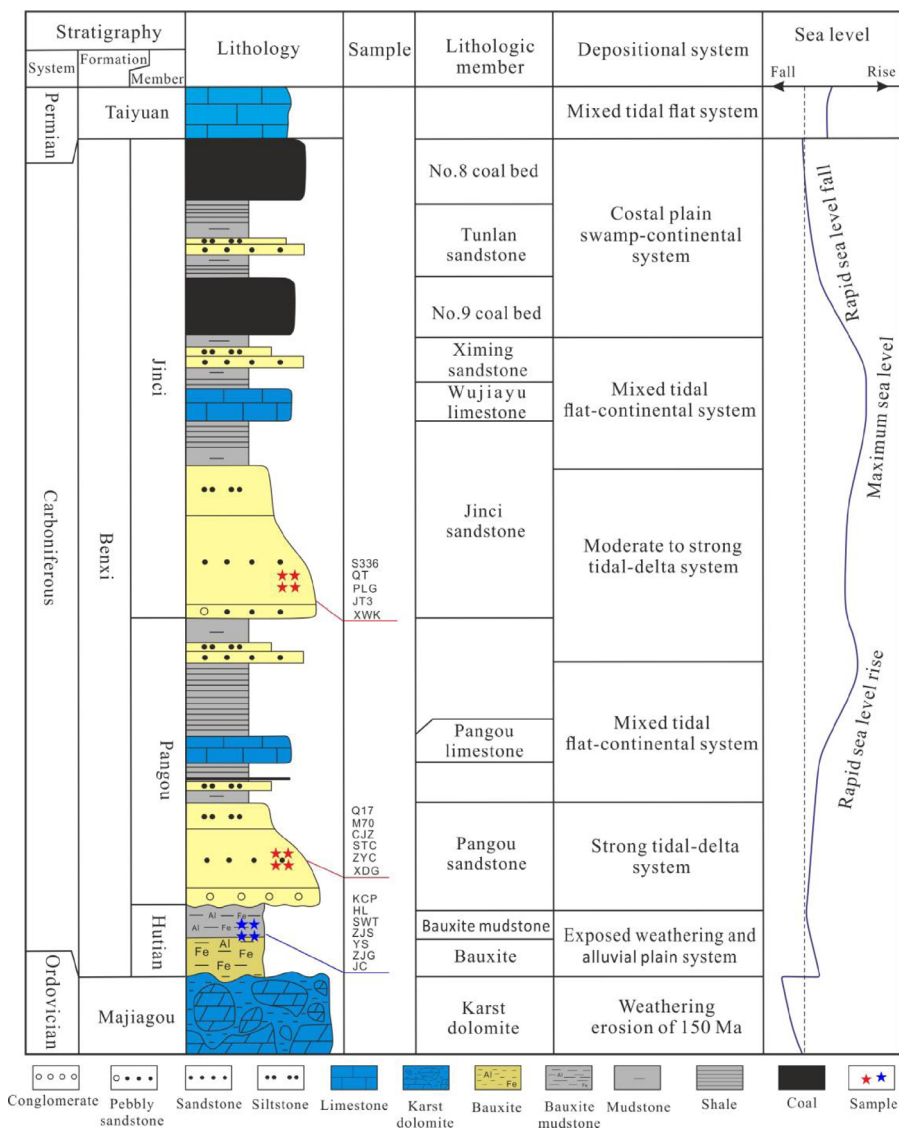


Figure 2. Comprehensive column diagram of Benxi Formation in North China Craton. The samples taken from XDG, ZYC, STC, CJZ, M70, and Q17 are located in the Pangou member. The samples taken from XWK, JT3, PLG, QT, and S336 are located in the Jinci member. The samples taken from KCP, HL, SWT, ZJS, YS, ZJG, JC [Cai, 2014] and ZJS [Wang et al., 2016] are located in the Hutian member.

Palaeozoic, and its thickness primarily depended on paleotopography. It was generally thick-bedded at the depressed zone and thin-bedded or even absent at the high platform zone, ranging from 5 to 120 m. In general, the total thickness thins from north to south.

The Benxi Formation is divided into three members (Figure 2), Hutian, Pangou, and Jinci, in

ascending order. The Hutian member is composed of a set of grey, grey-white bauxite, and bauxite mudstone, which is generally considered as the weathered crust mudstone or swamp mudstone deposit in the alluvial plain [Chen et al., 2010, Shao et al., 2014, Hou et al., 2018, Jia et al., 2019, Li et al., 2014, Shao et al., 2014]. The Pangou member is composed of sandstone, conglomerate, siltstone, mudstone-shale,

coal, and limestone. The conglomerate contains quartz gravels that are moderately sorted and well or poorly rounded. Conglomerate is developed in the southern and southwestern parts of the Ordos Block, while conglomerate in the northern part is quite rare. The Jinci member contains a grey-white, grey-green, and grey-brown quartz sandstone at the bottom, the limestone in the middle, and the No. 8 and No. 9 coal beds at the top.

The clastic composition of the Benxi Formation sandstone and conglomerate is dominated by quartz and a small amount of metamorphic rock clasts in the north-eastern part of the Ordos Block, and by quartz, metamorphic rock clasts, and a small amount of sedimentary rock and volcanic rock debris in the southern part. The Benxi Formation sandstone in the northern part of the Ordos Block is usually blue-coloured under cathodoluminescence, implying the parent rock of igneous rocks. In the southern part, quartz particles are commonly dark brown, implying the parent rock of metamorphic rocks [Jia *et al.*, 2019].

4. Sample and analysis method

Detrital zircon can be used to trace the source rocks due to its abundance in the Benxi Formation sandstone. In this study, zircon U–Pb age-dating was carried out using sandstone samples collected at the Xiaodonggou (XDG) area in Jincheng, Zhuyuancun (ZYC) area in Hancheng, Xiweikou (XWK) area in Hejin, Shantoucun (STC) area in Puxian, Well Jitan-3 (JT3), Well Shan-336 (S336), Well Mi-70 (M70), Well Qi-17 (Q17), Chengjiazhuang (CJZ) area in Liulin, Palougou (PLG) area in Baode, and Qiaotou (QT) area in Baode (Figure 1). Sampling locations are displayed in Figures 1 and 2. The main rock type of the samples is quartz sandstone and a small amount of lithic quartz sandstone; feldspar is hardly developed. The samples contain 76–92% quartz, 6–20% metamorphic rock debris, 1–3% sedimentary rock debris, and 1% magmatic rock debris [Jia *et al.*, 2019]. Next, cathodoluminescence (CL) of detrital zircons was conducted. The morphological characteristics of detrital zircon were analysed under the condition that fracture and inclusion are avoided. In each sample, 100 points were selected for U–Pb age-dating. Meanwhile, Hf isotopic measurements were conducted for six samples, XDG, ZYC, XWK, STC, CJZ, and QT.

Zircon grains were separated by grinding the samples to 40 mesh sizes (420 μm) and then using conventional heavy liquid and magnetic techniques, followed by hand-picking under a binocular microscope. Their internal structures were documented using cathode luminescence (CL) images. The CL images were then used to select targets for U–Pb isotopic analysis [Wang *et al.*, 2016]. Laser Ablation Multi-Collector Inductively Coupled Plasma Mass Spectrometry (LA-MC-ICP-MS) was used to analyse the selected detrital zircons for U–Pb ages and Hf isotopes. The selected zircon grains were analysed using a Nu Plasma II MC-ICP-MS equipped with an ASI RESOLUTION LR 193 nm ArF laser source in the State Key Laboratory of Continental Dynamics, Northwest University of China, following procedures reported in [Liu *et al.*, 2007]. The operating conditions and analytical procedures of Hf isotopes are reported in Hu *et al.* [2012]. We used the present-day chondrite values of $^{176}\text{Hf}/^{177}\text{Hf} = 0.282772$ and $^{176}\text{Lu}/^{177}\text{Hf} = 0.0332$ [Blichert-Toft and Albarède, 1997] to calculate $\varepsilon\text{Hf}(0)$, and the observed zircon U–Pb ages and the decay constant of ^{176}Lu ($1.865 \times 10^{-11} \text{ yr}^{-1}$; Scherer *et al.*, 2001) to calculate $\varepsilon\text{Hf}(t)$.

5. Result of detrital zircon U–Pb geochronology

5.1. Zircon morphology

Cathodoluminescence (CL) provides a clear reflection of the internal structure of zircons of different origins. Volcanic zircons show typical magma oscillating bands, of which the width can be influenced by crystallization temperature. Internal structure of metamorphic zircons can be complex and highly variable. Zircons formed under different metamorphic conditions have different internal structures, which include no-zonation, weak zonation, fan-shaped zonation, planar zonation, patchy zonation, sponge zonation, and flow zonation [Cai, 2014]. Zircons derived from sedimentary rocks are usually well sorted and abraded to some degree.

The diameter of detrital zircon crystals chosen for this study ranges from 60 to 280 μm , with the majority ranging from 90 to 140 μm . Cathodoluminescence images (Figure 3) reveal that the majority of detrital zircon crystals have evident oscillating zone texture, and the oscillating zone width is

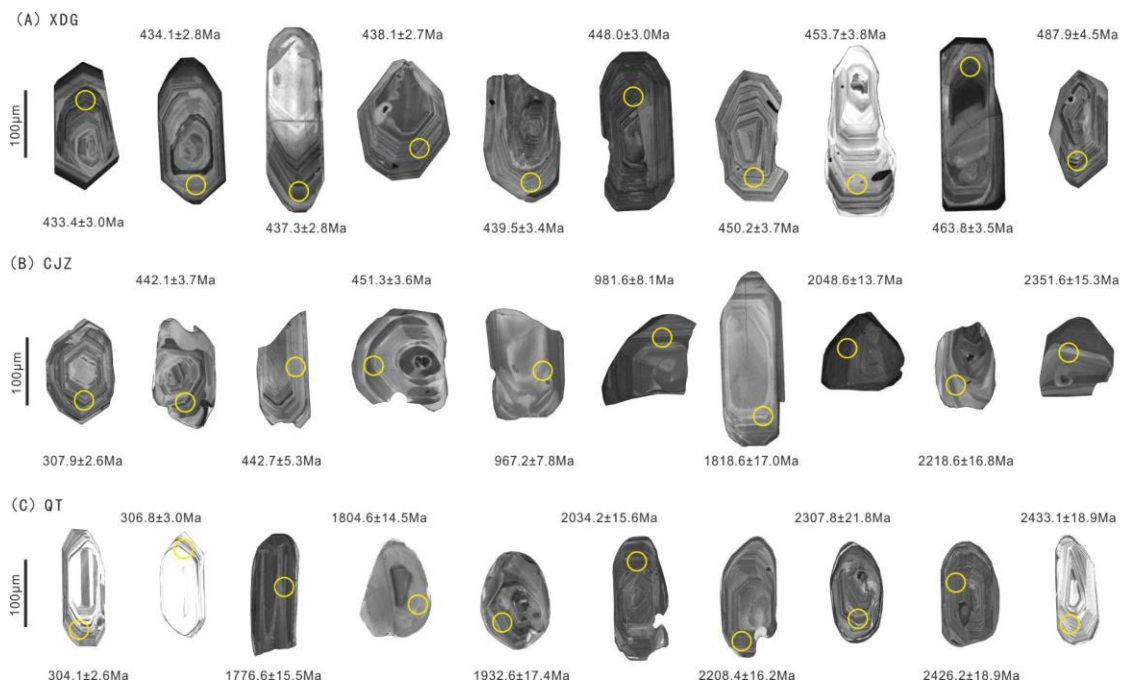


Figure 3. Cathodoluminescence (CL) images of detrital zircons in sandstone samples taken from Benxi formation in the North China Craton. Circles are the analytical targets.

relatively small in most zircon crystals and large in only very few crystals. Some zircon particles exhibit wide oscillating zones or no-zone properties. A few zircon crystals show irregular characteristic oscillating zones or no-zone, and some exhibit the core and mantle structure. Zircon crystals under the transmitted light are mostly euhedral, vary greatly in size, and exhibit evident edges and a well-preserved crystal form. A few zircons with relatively small grain sizes are highly rounded. Abrasion of different degrees can be observed on the zircon crystal face. A few zircons are severely abraded on the crystal face, crystals are crushed, and fractures are formed.

5.2. Zircon U–Pb ages

In this study, if the $^{206}\text{Pb}/^{238}\text{U}$ age is less than 1000 Ma, the zircon age equals to the $^{206}\text{Pb}/^{238}\text{U}$ age; if the $^{206}\text{Pb}/^{238}\text{U}$ age is greater than 1000 Ma, the zircon age equals to the $^{207}\text{Pb}/^{206}\text{U}$ age. Detrital zircons in sandstone samples collected at the Benxi Formation show six peak ages (Figures 4, 5), ca. 310, 450, 800, 950, 1900, and 2500 Ma. Zircons in the sandstone samples (CJZ, M70, Q17) taken from the central part

of the NCC exhibit six peaks. Zircons in the sandstone samples (QT, PLG) taken from the northern part of the NCC show peaks around 310, 1900, and 2500 Ma, and without any peaks of around 450, 800, or 950 Ma. Zircons in the sandstone samples (XDG, ZYC, XWK, JT3, STC, and S336) taken from the southern part of the NCC do not contain zircons of ca. 310 Ma, but all have a prominent peak at ca. 450 Ma.

5.3. Zircon Hf isotopes

Figure 6 A, B, and C illustrate the variations in detrital zircon $\epsilon\text{Hf}(t)$ values among the studied bauxite [Wang *et al.*, 2016] and sandstone deposits in the NCC. Detrital zircons with the U–Pb age close to 450 Ma from the NCC have $\epsilon\text{Hf}(t)$ values ranging from +15 to –10. The highest $\epsilon\text{Hf}(t)$ values are comparable to that of the depleted mantle, suggesting the occurrence of a juvenile crust formed at ca. 450 Ma in the source region of detrital zircons. Some zircon grains have strongly negative $\epsilon\text{Hf}(t)$ values, suggesting a source formed by reworking of old crustal materials. Detrital zircons with peak ages of ca. 310 Ma from the northern and central parts the NCC have

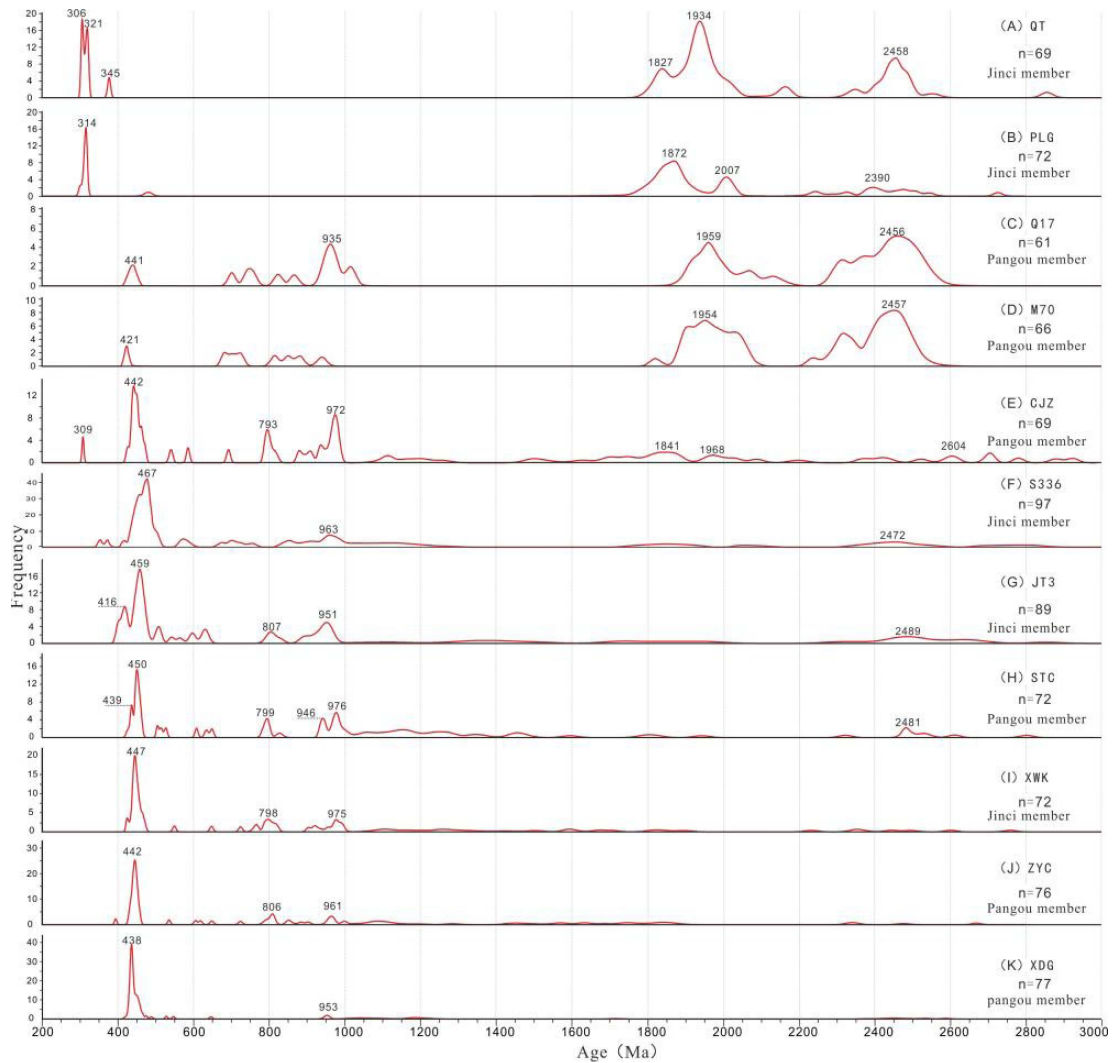


Figure 4. Histograms of detrital zircon U–Pb ages for typical sandstone samples taken from Benxi Formation in the North China Craton. (A) Samples QT; (B) PLG; (C) Q17; (D) M70; (E) CJZ; (F) S336; (G) JT3; (H) STC; (I) XWK; (J) ZYC; and (K) XDG.

a rather restricted range of $\varepsilon_{\text{Hf}}(t)$ values from +2 to –10.

6. Discussion

A few past studies [Cai, 2014, Wang *et al.*, 2016] investigated the zircon U–Pb age-dating of the bauxite samples taken from the Hutian member of the Benxi Formation in the NCC (Figure 6). The results indicated that the age of zircons in the bauxite peaked at

ca. 320, 450, 950, 1900, and 2500 Ma. All the samples peaked at ca. 450 Ma. Bauxite contains more zircons of ca. 320 Ma in the central and northern parts of the NCC than in the southern part. The age of zircons in the sandstone samples taken from the northern part of the NCC peaked at ca. 310, 1900, and 2500 Ma (Figures 4, 5).

The comparison of the age spectrum of zircon in bauxite and sandstone taken from the Benxi Formation with that in igneous and metamorphic rocks of

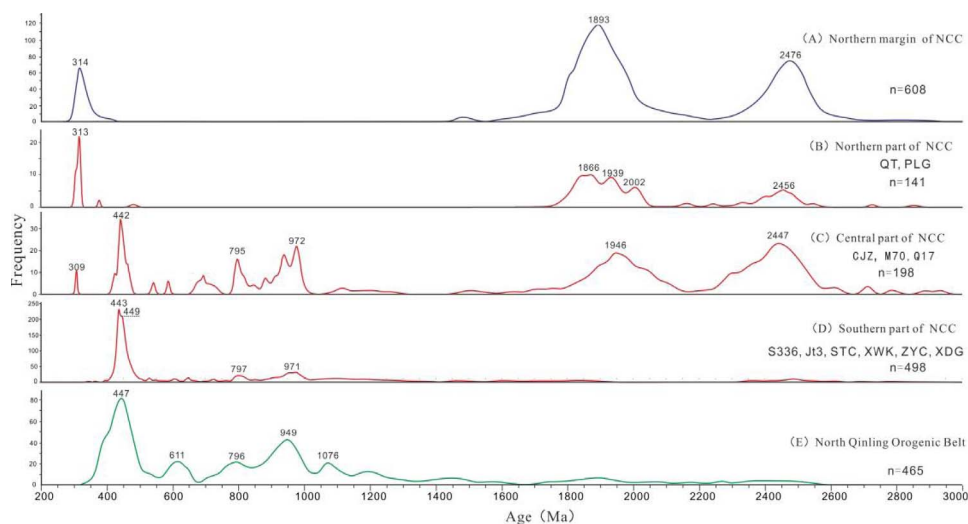


Figure 5. Comparison of zircon U–Pb ages for the southern, central, and northern parts of the North China Craton. (A) The ages for the northern margin of the North China Craton are from Wan *et al.* [2006], Zhang *et al.* [007a,b], He *et al.* [2009]. (E) The ages for the North Qinling Orogenic Belt are from Zhang [2008], Zhu *et al.* [2011] and Di Wu *et al.* [2010].

the North Qinling Orogenic Belt, Bainaimiao arc, and northern margin of NCC shows peaks around 2500, 1900, 950, 800, 450, and 310 Ma (Figure 5). The age of detrital zircons in sandstone (CJZ) in the central part of the NCC is ca. 450 Ma, with the exception of only one zircon of ca. 310 Ma (Figure 4). However, more zircons of ca. 320 Ma are present in the bauxite [Cai, 2014, Wang *et al.*, 2016] (Figure 6). By contrast, detrital zircons in sandstone samples (PLG and QT) taken from the central and northern parts of the NCC exhibit clear peak ages of ca. 310, 1900, and 2500 Ma, but no peak age of ca. 450 Ma (Figure 4). However, detrital zircons of ca. 320 and 450 Ma are present in the bauxite [Cai, 2014, Wang *et al.*, 2016] (Figure 6). These differences suggest that the provenance of the Benxi Formation may vary across the NCC.

6.1. Origin of detrital zircons

Zircons in rock samples taken from the North Qinling Orogenic Belt show three peak ages of 400–500 Ma, 750–850 Ma, 900–1000 Ma, and no peak ages of 300–330 Ma, 1800–2000 Ma, and 2300–2600 Ma (Figure 5). Detrital zircons in the Benxi Formation (including sandstone and bauxite) with peak ages of ca. 1900 and ca. 2500 Ma taken from the central and

northern parts of the NCC share similar $\varepsilon_{\text{Hf}}(t)$ values with the those formed in the same period taken from the northern margin of the NCC (Figure 7). This suggests that detrital zircons in the Benxi Formation originated from the northern margin of the NCC, and that the northern margin of the NCC began to uplift in the Late Carboniferous.

Magmatism of ca. 800 and ca. 950 Ma is contained at the North Qinling Orogenic Belt. Detrital zircons in the Benxi Formation with the peak ages of ca. 800 and ca. 950 Ma share similar $\varepsilon_{\text{Hf}}(t)$ with the igneous and metamorphic zircons formed at the same period taken from the North Qinling Orogenic Belt (Figure 7), suggesting that this type of zircon originated from the North Qinling Orogenic Belt.

Peak age of ca. 450 Ma exists in all bauxite samples taken from the Hutian member of the Benxi Formation in the NCC. In sandstone samples (Pangou, Jinci member), only the peak age of ca. 450 Ma exists in the southern central part of the NCC, but not in the northern part, indicating that the paleotopography of the intercontinental plate in the NCC has considerable changes. Palaeozoic igneous rocks formed in the North Qinling Orogenic Belt show $\varepsilon_{\text{Hf}}(t)$ values from +15 to –10 and the peak age of zircons in Palaeozoic igneous rocks ranges from 400 to 500 Ma

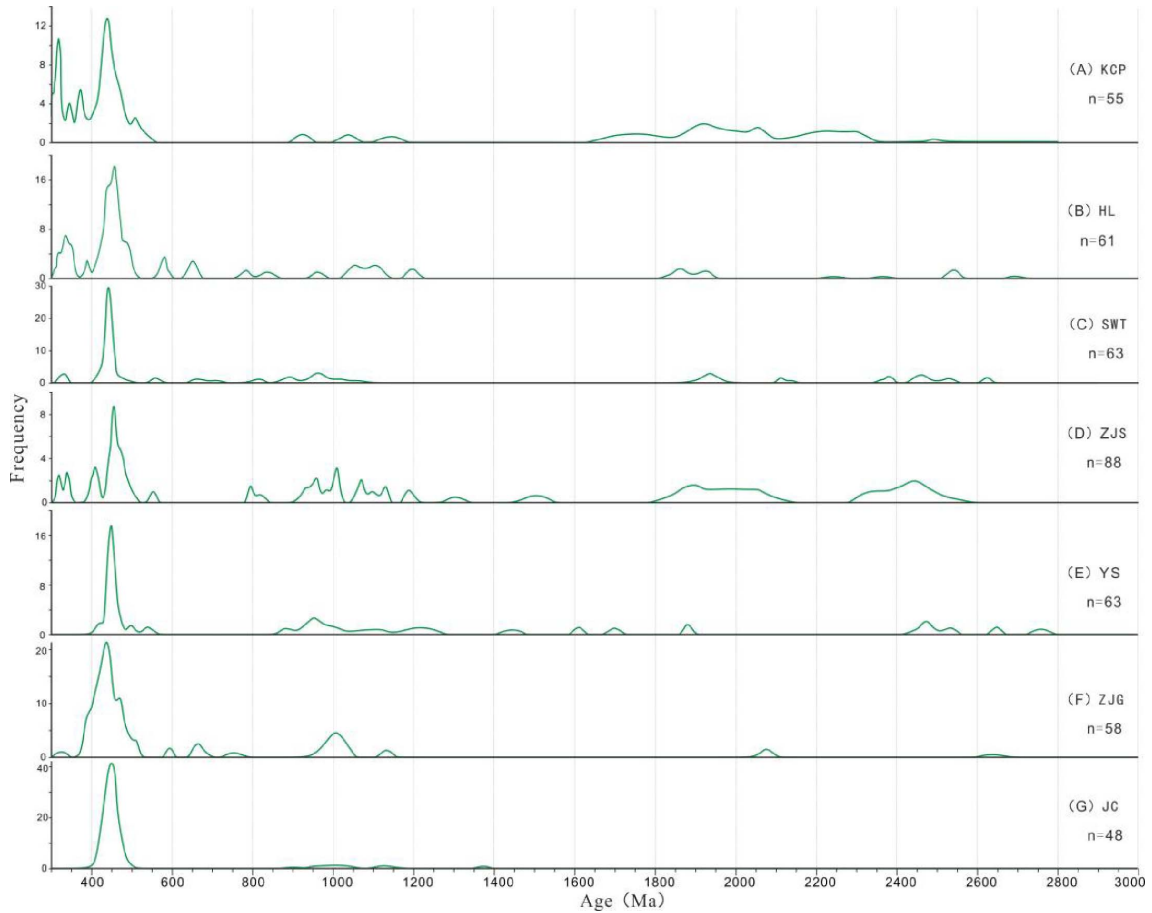


Figure 6. Histograms of detrital zircon U–Pb ages for typical bauxite samples taken from Hutian member of Benxi Formation in the North China Craton. (A) Samples KCP; (B) HL; (C) SWT; (D) ZJS; (E) YS; (F) ZJG; and (G) JC. The ages for KCP, HL, SWT, YS, ZJG and JC are from Cai [2014]. The ages for ZJS is from Wang *et al.* [2016].

(Figure 7), with a peak at 450 Ma, indicating that the occurrence of subduction during 400–500 Ma resulted in the reconstruction of ancient crust and the formation of younger crust. Zircons with the peak age of 400–500 Ma taken from Palaeozoic igneous rocks in the North Qinling Orogenic Belt have $\epsilon_{\text{Hf}}(t)$ values ranging from negative to positive values. Conversely, the majority of zircons of the same peak age taken from intrusive and sedimentary rocks in the southern part of the Central Asian Orogenic Belt are positive (Figure 7), which are significantly different from those of contemporaneous detrital zircons taken from the Carboniferous Benxi Formation. Accordingly, the majority of detrital zircons with

the peak age of ca. 450 Ma in the Benxi Formation originated from the North Qinling Orogenic Belt, rather than the Bainaimiao arc in the southern part of the Central Asian Orogenic Belt. It is highly likely that these zircons were transported by hydrodynamic processes rather than volcanic eruption. During the collision between the North Qinling arc and the south margin of North China Craton (>430 Ma), Erlangping back arc basin was uplifted and erode, and the intrusive rocks in the basin were also weathered and erode, which provided detrital zircons for the deposition of North China Craton [Cai, 2014].

The Late Carboniferous igneous rocks rarely developed in the North Qinling Orogenic Belt but were

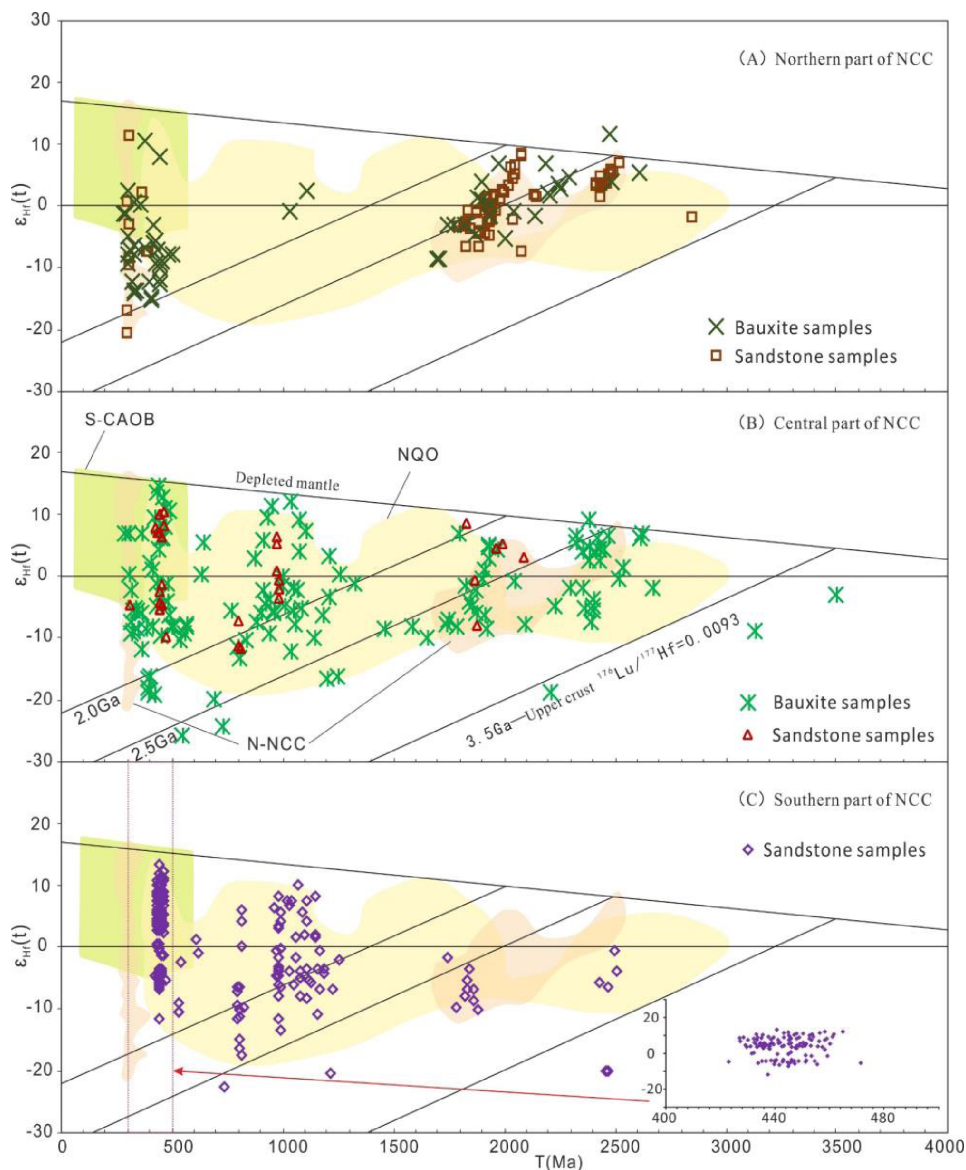


Figure 7. Plot of $\epsilon_{\text{Hf}}(t)$ versus age (Ma) for the detrital zircons in the bauxite and sandstone samples of Benxi Formation in the North China Craton. Data for the bauxite samples are from Wang *et al.* [2016]. The $\epsilon_{\text{Hf}}(t)$ ranges of detrital zircons from possible source regions are also shown. Data for the S-CAOB (southernmost part of the Central Asian Orogenic Belt) and the northern margin of the NCC (North China Craton) are from Yang *et al.* [2006] and Zhang *et al.* [007a,b], and those for the NQO (North Qinling Orogenic Belt) are from Shi *et al.* [013a,b].

commonly present in the northern margin of the NCC. The ca. 310 Ma detrital zircons taken from the Benxi Formation in the central and northern parts of the NCC share similar $\epsilon_{\text{Hf}}(t)$ values with

those taken from the igneous rocks in the same period in the northern margin of the NCC, which are mostly negative (Figure 7). This suggests that the ca. 310 Ma detrital zircons originated from the

northern margin of the NCC and might be transported by hydrodynamic processes due to the large distance between the provenance and the final deposition.

6.2. *Tectonic-depositional setting*

The inferred derivation of the ca. 450 Ma detrital zircons in the bauxite deposits across the NCC from the North Qinling Orogenic Belt implies that the surface of the craton had an overall north-dipping topography and a prominent mountain along the southern margin of the craton [Wang *et al.*, 2016]. The ca. 450 Ma detrital zircons in sandstone samples taken from the Jinci and Pangou members of the Benxi Formation only exist in the southern and central parts of the NCC, but not in the northern part of the NCC. The bauxite and sandstone samples taken from the northern and central parts of the NCC are rich in ca. 320 Ma [Cai, 2014, Wang *et al.*, 2016] and ca. 310 Ma detrital zircons. This indicates that the surface of the northern part of the NCC had changed from north-dipping to south-dipping topography due to the effect of rapid uplifting of the northern margin.

In response to the south-dipping topography, the weathered products in the northern margin of the NCC began to migrate towards south. Therefore, the changes in the source of these detrital zircons occurred during the late sedimentary period of the Hutian member of the Upper Carboniferous Benxi Formation.

The NCC witnessed a sedimentary hiatus of ca. 150 Ma from the Middle Ordovician to the Late Carboniferous. Therefore, the North Qinling arc and the Bainaimiao arc are less likely to develop directly at the margin of the NCC. It is highly likely that these arcs are actually part of the Palaeozoic distal arc system or the drift arc terrane that coexisted with the Craton at its margin during the Late Carboniferous. The Palaeozoic Erlangping back-arc basin is present between the North Qinling arc and the NCC, which reveals its consistency with the Palaeozoic arc terranes and suggests that the collision between these arc terranes and the NCC occurred prior to ca. 430 Ma. The structural evolution of the southern Central Asian Orogenic Belt is in accordance with an alternative multiple orogenic model [Zhang *et al.*, 2018]. In the Early Palaeozoic, a trench-arc system (500–410 Ma) was developed in the Paleo-Asian-Ocean,

and the Bainaimiao arc was formed. In the Devonian, the closure of the Paleo-Asian-Ocean led to the collisional orogeny (ca. 400 Ma), and the collision between the Bainaimiao arc and the NCC. In the Carboniferous-Permian, the intracontinental extension resulted in the formation of limited ocean basins (350–250 Ma). The Bainaimiao arc was reactivated and the magmatism related to the extension was widely developed. In the Early-Middle Triassic, the passive closure of the limited ocean basin resulted in intraplate orogeny (ca. 240 Ma).

Prior to the Devonian, the northern and southern margins of the NCC made up the active continental margin, which was bordered to the south by the North Qinling arc and to the north by the south-drifting Bainaimiao arc. The convergence of these Palaeozoic arc terrane systems and the NCC occurred during the late sedimentary period of the Hutian member of the Carboniferous Benxi Formation (ca. 310 Ma), leading to a significant change in topography over the entire intracontinental plate. Based on the analysis results of gravel and light mineral cathodoluminescence [Jia *et al.*, 2019], lithofacies paleogeography [Chen *et al.*, 2010, Hou *et al.*, 2018, Shao *et al.*, 2014], paleotopography unit on the paleoerosional surface [Gan, 1984, Lü *et al.*, 2010], and marine transgression events [Wu *et al.*, 1995, Chen, 1998] for the Benxi Formation in the NCC, the North Qinling Orogenic Belt during the early sedimentary period of the Benxi Formation Hutian member was uplifted and eroded rapidly and developed into a major provenance; the paleotopography was south-uplifting and north-dipping (Figure 8a). From the late sedimentary period of the Hutian member (Figure 8b) to the sedimentary period of the Pangou (Figure 9a) and Jinci members (Figure 9b), structural inversion enabled the northern margin of the NCC to uplift rapidly and erode, the paleotopography was north-uplifting and south-dipping, and two distinct provenances were present in the sediments of the Benxi Formation. The sediments were supplied predominantly by the provenance in the north (Figure 9).

7. Conclusions

The Upper Carboniferous sediments of the Benxi Formation in the North China Craton (NCC) have two distinct provenances. In the early sedimentary

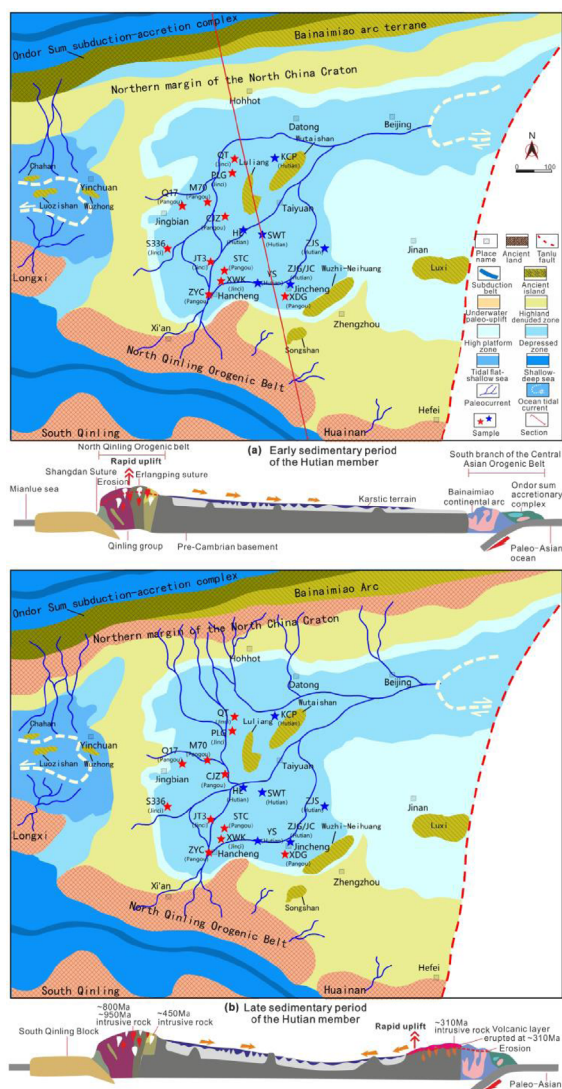


Figure 8. Proposed model for tectonic evolution and associated paleogeographic changes in the North China Craton during the sedimentary period of the Hutian member (Benxi Formation). (a) Shows the northern part of the Qinling Orogenic Belt uplifted quickly, and the paleotopography of the North China Craton was north-dipping. These induced the input of weathered rock material from the North Qinling Orogenic Belt to the North China Craton. (b) Shows the structural inversion enabled the northern margin of the North China Craton changed into south-dipping. Geological cross section model revised from Wang et al. [2016]. The fluvial systems and tidal currents in the paleogeographic diagrams revised from Wu et al. [1995], Chen [1998], Chen et al. [2010], Guo et al. [2010], Shao et al. [2014] and Hou et al. [2018]. The paleotopography units on the paleoerosional surface revised from Gan [1984] and [Lü et al., 2010].

period of the Hutian member of the Benxi Formation, the North Qinling Orogenic Belt was rapidly uplifted, and the sediments in the NCC were mainly derived from the North Qinling Orogenic Belt. From the

late sedimentary period of the Hutian member to the sedimentary period of the Jinci member, structural inversion enabled the northern margin of the NCC to uplift rapidly, the paleotopography was

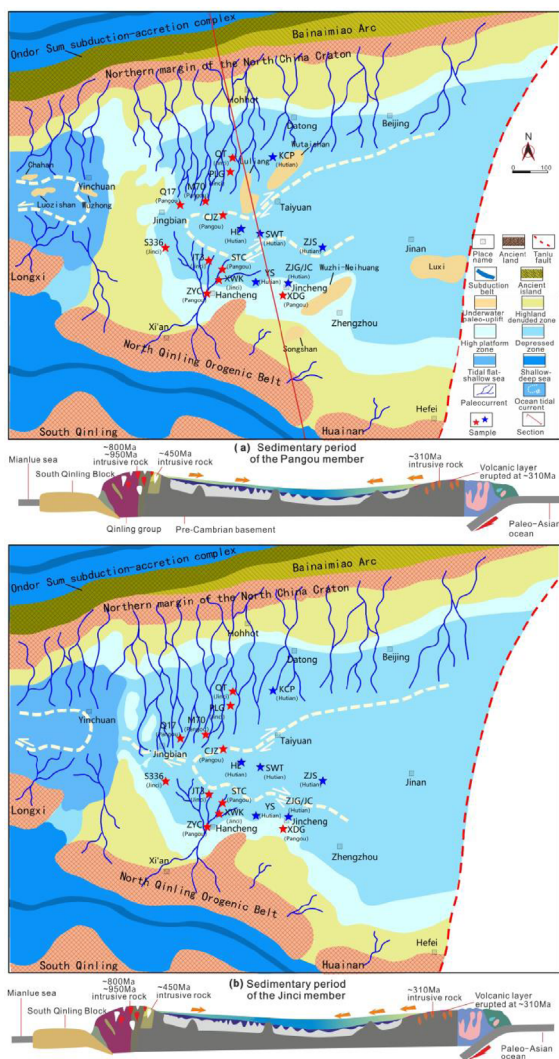


Figure 9. Proposed model for tectonic evolution and associated paleogeographic changes in the North China Craton during the sedimentary period of the Pangou–Jinci members (Benxi Formation). (a) and (b) Shows the northern margin of the North China Craton further uplifted, which induced the input of weathered material from the North Qinling Orogenic Belt and the northern margin of the North China Craton to the North China Craton. Geological cross section model revised from Wang et al. [2016]. The fluvial systems and tidal currents in the paleogeographic diagrams revised from Wu et al. [1995], Chen [1998], Chen et al. [2010], Guo et al. [2010], Shao et al. [2014] and Hou et al. [2018]. The paleotopography units on the paleoerosional surface revised from Gan [1984] and Lü et al. [2010].

north-uplifting and south-dipping. The Bainaimiao arc was reactivated, which resulted in the associated paleotopography change in the large Palaeozoic inland basin. The sediments of the Benxi Formation in the NCC were supplied predominately by the northern provenance.

References

Blichert-Toft, J. and Albarède, F. (1997). The Lu-Hf geochemistry of chondrites and the evolution of the mantle-crust system. *Earth Planet. Sci. Lett.*, 148:243–258.

- Cai, S. H. (2014). Detrital zircon geochronology and its implications. The Carboniferous bauxite deposits in the North China Craton. Master Thesis, China University of Geosciences China: 1–57 (in Chinese with English abstract).
- Cawood, P. A., Hawkesworth, C. J., and Dhuime, B. (2012). Detrital zircon record and tectonic setting. *Geology*, 40:875–878.
- Chen, J. L., Li, H. B., Wang, H. L., He, S. P., Zeng, Z. X., Xu, X. Y., and Li, X. M. (2007). LA-ICP-MS zircon U-Pb dating of a quartz diorite pluton from Wangjiacha, the junction area between the Qinling and Qilian orogenic belts and its tectonic significance. *J. Jilin Univ. (Earth Science Edition)*, 37:423–431.
- Chen, Q. H., Li, K. Y., Zhang, D. F., Jin, S. L., Guo, Y. Q., Pang, J. G., and Yuan, Z. (2010). The relationship between fan delta and hydrocarbon accumulation in Benxi-Taiyuan Formation, Ordos Basin. *Geol. China*, 37(2):421–429. (in Chinese, with English abstract).
- Chen, S. Y. (1998). The controls of the collisional orogenesis in the Qinling Mountains on the Carboniferous-Permian transgressional processes in North China. *Sedimentary Facies Palaeogeogr.*, 18(2):48–54. (in Chinese, with English abstract).
- De Jong, K., Xiao, W. J., Windley, B. F., Masago, H., and Lo, C. H. (2006). Ordovician $^{40}\text{Ar}/^{39}\text{Ar}$ phenigite ages from the blueschist-facies Ondor Sum subduction-accretion complex (Inner Mongolia) and implications for the early Palaeozoic history of continental blocks in China and adjacent areas. *Am. J. Sci.*, 306:799–845.
- Deng, J., Wang, Q. F., Yang, S. J., Liu, X. F., Zhang, Q. Z., Yang, L. Q., and Yang, Y. H. (2010). Genetic relationship between the Emeishan plume and the bauxite deposits in western Guangxi, China: constraints from U-Pb and Lu-Hf isotopes of the detrital zircons in bauxite ores. *J. Asian Earth Sci.*, 37:412–424.
- Di Wu, C. R., Sun, Y., Lin, C. L., Lin, C. L., and Wang, H. L. (2010). LA-(MC)-ICPMS U-Pb zircon geochronology and Lu-Hf isotope compositions of the Taihua complex on the southern margin of the North China Craton. *Sci. Bull.*, 55(23):2557–2571.
- Faure, M., Trap, P., Lin, W., Monié, P., and Bruguier, O. (2007). Polyorogenic evolution of the Paleoproterozoic Trans-North China Belt—New insights from the Lüliangshan-Hengshan-Wutaishan and Fuping massifs. *Episodes*, 30(2):96–107.
- Gan, D. Q. (1984). Analysis of mineralization of sedimentary bauxites of the North China platform. *Acta Sedimentologica Sin.*, 2(2):67–79. (in Chinese, with English abstract).
- Guo, C. L., Chen, D. L., Fan, W., and Wang, A. G. (2010). Geochemical and zircon U-Pb chronological studies of the Manziying granite in Erlangping area, western Henan province. *Acta Petrol. Et Mineral.*, 29:15–22. (in Chinese, with English abstract).
- He, Y. H., Zhao, G. C., Sun, M., and Xia, X. P. (2009). SHRIMP and LA-ICP-MS zircon geochronology of the Xiong'er volcanic rocks: implications for the Paleo-Mesoproterozoic evolution of the southern margin of the North China Craton. *Precambrian Res.*, 168(3–4):213–222.
- Hou, Y. D., Chen, A. Q., Zhao, W. B., Dong, G. D., Yang, S., Xu, S. L., Gao, Z. D., Li, F. X., Liu, X. X., and Zhang, X. X. (2018). Analysis on the depositional environment of Carboniferous Benxi Formation tidal-delta sand body complex, Ordos Basin, China. *J. Chendu Univ. Technol. (Science & Technology Edition)*, 45(4):393–401. (in Chinese, with English abstract).
- Hu, Z. C., Liu, Y. S., Gao, S., Liu, W. G., Yang, L., Zhang, W., Tong, X. R., Lin, L., Zong, K. Q., Li, M., Chen, H. H., and Zhou, L. (2012). Improved in situ Hf isotope ratio analysis of zircon using newly designed X skimmer cone and Jet sample cone in combination with the addition of nitrogen by laser ablation multiple collector ICP-MS. *J. Anal. At. Spectrom.*, 27:1391–1399. (in Chinese, with English abstract).
- Jia, L. B., Zhong, D. K., Sun, H. T., Yan, R. T., Zhang, C. L., Mo, W. L., Qiu, C., Dong, Y., Li, B., and Liao, G. X. (2019). Sediment provenance analysis and tectonic implication of the Benxi Formation, Ordos Basin. *Acta Sedimentologica Sin.*, 37(5):1087–1103. (in Chinese, with English abstract).
- Jiang, S. H., Nie, F. J., Fang, D. H., and Liu, Y. F. (2009). Geochronology and geochemical features of the main intrusive rocks in the Weishancheng area, Tongbai County, Henan. *Acta Geol. Sin.*, 83:11–1029. (in Chinese, with English abstract).
- Lerch, M. F., Xue, F., and Kroner, A. (1995). A Paleozoic magmatic arc in the Heihe area, Qinling orogenic belt, central China. *J. Geol.*, 103:437–449.
- Li, N., Sun, Y. L., Li, J., Xue, L. W., and Li, W. B. (2008). Molybdenite Re-Os isotope age of the Dahu Au-Mo deposit, Xiaoqinling and the indosinian mineral-

- ization. *Acta Petrol. Sin.*, 24:810–816. (in Chinese, with English abstract).
- Li, W. B., Zhong, R. C., Xu, C., Song, B., and Qu, W. J. (2012). U-Pb and Re-Os geochronology of the Bainaimiao Cu-Mo-Au deposit, on the northern margin of the North China Craton, North Asia Orogenic Belt: implications for ore genesis and geodynamic setting. *Ore Geol. Rev.*, 48:139–150.
- Li, Y. (2011). Paleozoic ophiolites and tectonic evolution of the North Qinling. Master Thesis, Chinese Academy of Geological Science; 1–140 (in Chinese, with English abstract). *Ore Geology Reviews*.
- Li, Y., Zhang, J. W., Li, J., He, J., Sun, G. M., and Qiao, Y. L. (2014). A study on sedimentary microfacies of Benxi Formation and its controlling effect on gas enrichment in Yanchang district of Ordos Basin. *Northwestern Geol.*, 47(2):216–222. (in Chinese, with English abstract).
- Liu, J. F., Sun, Y., and Zhang, H. (2007). Zircon age of Luohansi group in the northern Qinling and their geological significance. *J. Northwest Univ. (Natural Science Edition)*, 37(6):907–911. (in Chinese, with English abstract).
- Lü, D. W., Wei, X. W., Liu, H. Y., and Liu, B. B. (2010). Classification of paleogeomorphology units and law of coal accumulation in Late Carboniferous of the North China Plate. *Petrol. Geol. Recovery Efficiency*, 17(5):24–28. (in Chinese, with English abstract).
- Lu, S. N., Li, H. K., Chen, Z. H., Hao, G. J., Zhou, H. Y., Guo, J. J., Niu, G. H., and Xiang, Z. Q. (2003). In *Meso-Neoproterozoic Geological Evolution of the Qinling and its Response to Rodinia Event*, pages 1–167. Geological Publishing House, Beijing.
- Mattauer, M., Matte, P., Malavielle, J., Tapponnier, P., Maluski, H., Xu, Z. Q., Lu, Y. L., and Tang, Y. Q. (1985). Tectonics of Qinling belt: built-up and evolution of eastern Asia. *Nature*, 317:496–500.
- Meng, Q. R. and Zhang, G. W. (2000). Geologic framework and tectonic evolution of the Qinling orogen, central China. *Tectonophysics*, 323:183–196. (in Chinese, with English abstract).
- Pei, X. Z., Liu, Z. Q., Ding, S. P., Li, Z. C., Li, G. Y., Li, R. B., Wang, F., and Li, F. J. (2007). Zircon LA-ICP-MS U-Pb dating of the Gabbro from the Baihua igneous complex in Tianshui area, eastern Gansu, and its geological significance. *Adv. Earth Sci.*, 22:818–827.
- Scherer, E., Münker, C., and Mezger, K. (2001). Calibration of the lutetium-hafnium clock. *Science*, 293:683–687.
- Shao, L. Y., Dong, D. X., Li, M. P., Wang, H. S., Wang, D. D., Lu, J., Zheng, M. Q., and Cheng, A. G. (2014). Sequence-paleogeography and coal accumulation of the Carboniferous-Permian in the North China. *J. China Coal Geol.*, 39(8):1725–1733. (in Chinese, with English abstract).
- Shi, G. Z., Faure, M., Xu, B., Zhao, P., and Chen, Y. (2013a). Structural and kinematic analysis of the Early Paleozoic Ondor Sum-Hongqimelange belt, eastern part of the Altaids (CAOB) in Inner Mongolia, China. *J. Asian Earth Sci.*, 66:123–139.
- Shi, Y., Yu, J. H., and Santosh, M. (2013b). Tectonic evolution of the Qinling orogenic belt, Central China: new evidence from geochemical, zircon U-Pb geochronology and Hf isotopes. *Precambrian Res.*, 231:19–60.
- Sun, Y. (1991). The ancient ocean and Caledonian orogeny in the East Qinling. *Geol. Rev.*, 37:555–559.
- Tian, W. (2003). *The Regional Petrogenesis of Granitic Rocks From Eastern Qinling and its Implication to the Tectonic Environment*. Peking University.
- Wan, Y. S., Song, B., Liu, D. Y., Wilde, S. A., Wu, J. S., Shi, Y. R., Yin, X. Y., and Zhou, H. Y. (2006). SHRIMP U-Pb zircon geochronology of Palaeoproterozoic metasedimentary rocks in the North China Craton: evidence for a major Late Palaeoproterozoic tectonothermal event. *Precambrian Res.*, 149(3–4):249–271.
- Wang, Q. F., Deng, J., Liu, X. F., Zhao, R., and Cai, S. H. (2016). Provenance of Late Carboniferous bauxite deposits in the North China Craton: new constraints on marginal arc construction and accretion processes. *Gondwana Res.*, 38:86–98.
- Wang, T., Wang, X. X., Tian, W., Zhang, C. L., Li, W. P., and Li, S. (2009). North Qinling Paleozoic granite associations and their variation in space and time: implications for orogenic processes in the orogens of central China. *Sci. China (Series D)*, 52:1359–1384. (in Chinese, with English abstract).
- Wen, Z. L., Xu, X. Y., Zhao, R. F., Wang, F., and Hu, W. (2008). Geologic and geochemical features of Devonian granites in Dangchuan area, Western Qinling, and its tectonic significance. *Geol. Rev.*, 54:827–836. (in Chinese, with English abstract).
- Wu, F. D., Chen, Z. H., Zhang, S. L., and Ge, L. G. (1995). Marine transgression during

- Carboniferous-Permian in the North China Craton. *Geoscience*, 9(3):284–291. (in Chinese, with English abstract).
- Xu, B., Charvet, J., Chen, Y., Zhao, P., and Shi, G. Z. (2013). Middle Paleozoic convergent orogenic belts in western Inner Mongolia (China): framework, kinematics, geochronology and implications for tectonic evolution of the Central Asian Orogenic Belt. *Gondwana Res.*, 23(4):1342–1364.
- Xu, X. Y., He, S. P., Wang, H. L., Zhang, E. P., Chn, J. L., and Sun, J. M. (2008). Tectonic framework of North Qinling Mountain and North Qilian Mountain conjunction area in Early Paleozoic: a study of the evidences from strata and tectonic magmatic events. *Northwestern Geol.*, 41:1–21. (in Chinese, with English abstract).
- Xue, F., Kröner, A., Reischmann, T., and Lerch, M. F. (1996). Palaeozoic pre- and post-collision calc-alkaline magmatism in the Qinling orogenic belt, central China, as documented by zircon ages on granitoid rocks. *J. Geol. Soc.*, 153:409–417.
- Yan, Q. R., Chen, J. L., Wang, Z. Q., Yan, Z., Wang, T., Li, Q. G., Zhang, Z. Q., and Jiang, C. F. (2007). Tectonic setting and SHRIMP age of volcanic rocks in the Xieyuguan and Caotangou Group: implications for the North Qinling orogenic belt. *Acta Geol. Sin.*, 81:488–500. (in Chinese, with English abstract).
- Yang, Z., Dong, Y. P., Liu, X. M., and Zhang, J. H. (2006). LA-ICP-MS zircon U-Pb dating of gabbro in the Guanzizhen ophiolite, Tianshui, West Qinling, China. *Chin. Sci. Bull.*, 25:1321–1325.
- Zhai, M. G. (2007). Paleoproterozoic events in the North China Craton. *Acta Petrologica Sin.*, 23(11):2665–2682. (in Chinese, with English abstract).
- Zhang, H. (2008). *The Chronological Study on U-Pb Dating of Modern River Detrital Zircon in North Piedmont Qinling and its Geological Indication*. Northwest University. (in Chinese, with English abstract).
- Zhang, J. R., Wei, C. J., and Chu, H. (2018). New model for the tectonic evolution of Xing'an-Inner Mongolia Orogenic Belt: evidence from four different phases of metamorphism in Central Inner Mongolia. *Acta Petrol. Sin.*, 34(10):2857–2872. (in Chinese, with English abstract).
- Zhang, S. H., Zhao, Y., and Song, B. (2006a). Hornblende thermobarometry of the Carboniferous granitoids from the Inner Mongolia Paleouplift: implications for the tectonic evolution of the northern margin of North China block. *Mineral. Petrol.*, 87:123–141.
- Zhang, S. H., Zhao, Y., and Song, B. (2006b). *Isotopic Geochronology and Geochemistry of Ophiolites, Granites and Clastic Sedimentary Rocks in the Qinling Orogenic Belt*. Geological Publishing House, Beijing. (in Chinese, with English abstract).
- Zhang, S. H., Zhao, Y., Song, B., and Wu, H. (2004). The late Paleozoic gneissic granodiorite pluton in Early Pre-Cambrian high-grade metamorphic terrains near Longhua county in northern Hebei province, North China: result from zircon SHRIMP U-Pb dating and its tectonic implications. *Acta Petrologica Sin.*, 20:621–626. (in Chinese with English abstract).
- Zhang, S. H., Zhao, Y., Song, B., and Yang, Y. H. (2007b). Zircon SHRIMP U-Pb and in-situ Lu-Hf isotope analyses of a tuff from western Beijing: evidence for missing Late Paleozoic arc volcano eruptions at the northern margin of the North China block. *Gondwana Res.*, 12:157–165.
- Zhang, S. H., Zhao, Y., Song, B., Yang, Z. Y., Hu, J. M., and Wu, H. (2007a). Carboniferous granitic plutons from the northern margin of the North China block: implications for a late Paleozoic active continental margin. *J. Geol. Soc.*, 164:451–463.
- Zhang, X. H., Mao, Q., Zhang, H. F., Zhai, M. G., Yang, Y. H., and Hu, Z. C. (2011). Mafic and felsic magma interaction during the construction of high-K calc-alkaline plutons within a metacratonic passive margin: the Early Permian Guyang batholith from the northern North China Craton. *Lithos*, 125:569–591.
- Zhu, R. K., Xu, H. X., Deng, S. W., and Guo, H. L. (2007). Lithofacies palaeogeography of the Carboniferous in northern China. *J. Palaeogeogr.*, 9(1):13–24. (in Chinese, with English abstract).
- Zhu, X. Y., Chen, F. K., Li, S. Q., Yang, Y. Z., Nie, H., Siebel, W., and Zhai, M. G. (2011). Crustal evolution of the North Qinling terrain of the Qinling Orogen, China: evidence from detrital zircon U-Pb ages and Hf isotopic composition. *Gondwana Res.*, 20(1):194–204.